Infrared study of the magnetostructural phase transition in correlated CrN

J. Ebad-Allah,[1,2] B. Kugelmann,[1] F. Rivadulla,[3] and C. A. Kuntscher[1,*]

[1]*Experimentalphysik 2, Universität Augsburg, D-86135 Augsburg, Germany*
[2]*Department of Physics, Tanta University, 31527 Tanta, Egypt*
[3]*Centro de Investigación en Química Biolóxica e Materiais Moleculares (CIQUS)*
and Departamento de Química-Física, Universidade de Santiago de Compostela, 15782 Santiago de Compostela, Spain

We report on the pressure and temperature dependence of the electronic and vibrational properties of polycrystalline CrN studied by optical transmission and reflection measurements over the frequency range 0.012–2.48 eV. The optical conductivity spectrum of CrN at ambient conditions shows a phonon mode at ≈ 55 meV with a shoulder at ≈ 69 meV, a pronounced midinfrared absorption band centered at 123 ± 2 meV, and a high-energy absorption band at ≈ 1.5 eV. The absorption bands are discussed in terms of the charge-transfer insulator picture. Following the reflectance spectrum with increasing pressure, the activation of an additional phonon mode above 0.6 GPa indicates the occurrence of a pressure-induced structural phase transition. Furthermore, the absorption spectrum exhibits significant changes in the far-infrared range with decreasing temperature: The phonon mode shows a sudden broadening followed by a splitting below 270 K. These changes observed under pressure or while cooling down can be associated with the magnetostructural phase transition reported previously.

I. INTRODUCTION

Transition-metal nitrides provide remarkable properties such as high hardness, mechanical strength, wear and corrosion resistance, high-temperature oxidation resistance, and good chemical as well as thermal stability [1–3]. Furthermore, they have been used in semiconductor devices because of their relatively high electrical conductivity [1–4]. Among the nitrides, CrN is the only compound which does not have a ground state of cubic symmetry, making it especially interesting. At ambient conditions, CrN is in a paramagnetic phase with a cubic rock-salt structure similar to other transition-metal nitrides. At the Néel temperature T_N with values in the range 270–286 K reported in the literature [5–8], the material undergoes a magnetic phase transition to an ordered antiferromagnetic phase. The magnetic phase transition is accompanied by a structural phase transition from the cubic phase to an orthorhombic phase. Recently, it has been reported [9] that this magnetostructural phase transition could also be induced by applying pressure of ≈ 1 GPa at room temperature. The pressure-induced phase transition at ≈ 1 GPa was found to be accompanied by a reduction of the bulk modulus of about 25% and a 0.56–0.59% increase in the atomic density [9].

The electrical transport studies of CrN revealed discrepant results regarding the temperature dependence of the resistivity. Several transport studies on polycrystalline samples [10–12] and thin films grown on MgO (001) substrates [13] supported the semiconductor scenario in the whole temperature range below 400 K, indicating the existence of a band gap. In contrast, Constantin *et al.* observed a change from semiconductor to metallic behavior in the conductivity spectrum at T_N on a thin film of CrN, while the recent study of Quintela *et al.* [14] on a thin film of CrN reported a metallic-like behavior for the

annealed CrN thin film in the temperature range below 400 K, with a steep decrease of the resistivity at T_N associated with the magnetostructural phase transition. A metallic behavior was also observed in other resistivity studies in the temperature range below 300 K [5,15].

Theoretical works interpreted the observed magnetic, structural, and electronic properties of CrN in terms of charge ordering or Mott-insulating behavior, which is characteristic for correlated electron systems [16]. Theoretical calculations using the local spin-density approximation corrected by Hubbard Coulomb terms for the d electrons (LSDA+U) [17] supported the idea that CrN is close to a charge-transfer type insulator. Here, a spin separation of states near the Fermi level was reported, leading to opening up a small charge gap of less than 1 eV between the N $2p$-type bands and Cr $3d$-type bands. This small energy gap was suggested to be related to the measured optical charge gap of 0.64 eV extracted from the absorbance spectrum [13,18]. In contrast, the analysis of the dielectric constant determined from transmission and reflection measurements in broad frequency ranges (0.04–5 eV and 0.1–5 eV, respectively) indicated the presence of a small indirect band gap of 0.19 ± 0.46 eV at the Fermi level. This gap was attributed to the formation of local magnetic moments and electron interaction effects, suggesting that CrN is a Mott-Hubbard-type insulator [19].

Here, we report on the electronic and vibrational properties of polycrystalline CrN investigated by reflectance and transmission measurements in a broad frequency range 0.012–2.48 eV (100–20 000 cm^{-1}). The goal of our optical study was to verify the semiconducting character suggested by electronic transport measurements, with an energy gap smaller than 150 meV at ambient conditions [13,18–20]. Furthermore, absorption measurements for temperatures between 300 and 150 K as well as room-temperature reflectance measurements under high pressure up to 4.5 GPa were carried out to search for

*christine.kuntscher@physik.uni-augsburg.de

signatures of the expected temperature- and pressure-induced magnetostructural transition.

II. EXPERIMENT

The CrN powder was synthesized by ammonolysis of Cr_3S_4 at $800\,^\circ$C for 10 h; details on the powder preparation are reported in Refs. [10,11].

For the temperature-dependent transmittance studies, the CrN powder was mixed with CsI in a certain ratio; here we used 0.14% of CrN to prepare the CrN/CsI pellet. The mixture was pressed to a sintered pellet of about 50 μm thick. Then pellets of a mixture of CrN/CsI and of pure CsI were mounted on the holder of a cold-finger cryostat (Cryo Vac Konti-Mikro cryostat). CsI was chosen due to its transparent in the infrared frequency range. The actual temperature of the sample was measured by a sensor attached in direct vicinity of the pellets. We measured the intensity of the radiation transmitted by the CrN pellet, $I_s(\omega)$; as reference, the intensity $I_r(\omega)$ transmitted by a pure CsI pellet was used. The ratio $T = I_s(\omega)/I_r(\omega)$ is a measure of the transmittance of the sample, and the corresponding absorbance was calculated according to $A = \log_{10}(1/T)$.

The reflectance measurement at ambient conditions was conducted in the frequency range 0.012–2.48 eV (100–20 000 cm^{-1}) using a Bruker IFS 66v/S Fourier transform infrared (FT-IR) spectrometer with an infrared microscope (Bruker IR scope II) equipped with a $15\times$ magnification objective. We measured the intensity of the radiation reflected from a pure CrN pellet, $I_s(\omega)$; as reference we measured the intensity reflected from an Ag mirror, $I_r(\omega)$. The ratio $R = I_s(\omega)/I_r(\omega)$ is a measure of the reflectance of the sample. The real part of the optical conductivity σ_1 was obtained via Kramers Kronig (KK) transformation. Hereby, the reflectivity data were extrapolated to low frequencies based on a Lorentz fit. For the high-frequency extrapolation we used the x-ray atomic scattering functions [21]. Alternatively, we measured the UV range up to around 5 eV, then used the power law of $(1/\omega)$ to extrapolate the reflectivity data. By this way we estimated the error bars and found that the high-energy extrapolation affects the high-energy features of the obtained optical conductivity only slightly.

Pressure-dependent reflectance experiments were carried out at room temperature in the far-infrared frequency range. For the generation of pressures up to 4.5 GPa, a clamp diamond anvil cell (Diacell cryoDAC-Mega) equipped with type IIA diamonds, which are suitable for infrared measurements, was used. A small piece (lateral dimensions of about 160 μm $\times$ 150 μm, with a thickness of $\sim$50 μm) was cut from a pure CrN pellet and placed in the hole of a CuBe gasket. Finely ground CsI powder served as quasi-hydrostatic pressure transmitting medium. The pressure in the diamond anvil cell was determined *in situ* by the ruby luminescence method [22]. As reference, we used the intensity reflected from the CuBe gasket inside the DAC. All the pressure-dependent reflectance spectra refer to the absolute reflectance at the sample-diamond interface, denoted as R_{s-d}. Further information about the geometry of the reflectivity measurements can be found in our earlier publications [23,24].
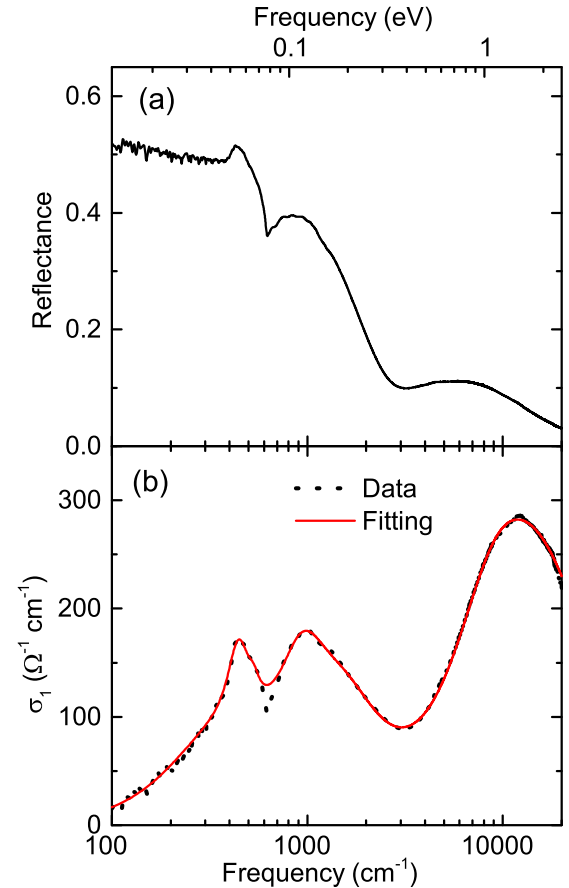

FIG. 1. (a) Reflectance of a pure CrN pellet over a broad frequency range at ambient conditions, used for the KK analysis to extract the optical conductivity. (b) Lorentz model fit of the corresponding real part σ_1 of the optical conductivity, obtained by KK analysis, at ambient conditions.

III. RESULTS AND DISCUSSION

A. Optical spectrum at ambient conditions

The ambient-condition reflectance spectrum of the pure CrN pellet over a broad frequency range and the corresponding real part σ_1 of the optical conductivity are depicted in Fig. 1. The reflectance spectrum consists of several contributions: a broad peak with a shoulder in the far-infrared range followed by a pronounced midinfrared (MIR) absorption band and a high-energy absorption band. For a quantitative analysis of the observed features, we fitted the optical conductivity σ_1 with the Lorentz model. The far-infrared peak and its shoulder were described by two Lorentzian functions. Furthermore, both the MIR band and the high-energy band were described by two Lorentzian functions each. Figure 1(b) shows the fit of the σ_1 spectrum with the Lorentz model. The finite conductivity in the far-infrared range does not give a clear indication of a Drude-type contribution, supporting a semiconducting behavior of CrN above T_N [10–13,25].

From the fitting we obtained the frequency position of the far-infrared peak at ≈ 55 meV. This peak is related to the transverse-optical (TO) mode predicted at 48.7 ± 0.2 meV [19]. The shoulder observed at around 69 meV could

be attributed to the predicted longitudinal optical mode located at 75.0 ± 6.8 meV [19]. Our results are slightly different from the previously published reflectance data, which show a broad phonon mode at around 52 meV [19]. The small difference in the position of the phonon mode could be attributed to the thickness, the composition, and the strain of the thin films used in the previous measurements, which affect the phonon mode position [20,26].

The MIR band located at 123 ± 2 meV can be attributed to a charge gap of size $\Delta \approx 100$–150 meV, consistent with the activated behavior observed by several resistivity studies which found activation energy E_a values in the range 50–75 meV [10–13,25]. Furthermore, we observe a high-energy band located at around 1.5 eV, in good agreement with the electronic interband transitions occurring at around 1.5 eV as observed by Zhang *et al.* [19].

In order to attribute the observed absorption bands to specific optical excitations, we will refer to the band-structure calculations of Herwadkar *et al.* using the LSDA+U approximation [17]. Here, for the cubic structure a strong depletion in the density of states by the spin separation of states near the Fermi level was predicted. A small gap between the N $2p$-type bands and Cr $3d$-type bands was found, suggesting that CrN is likely to be a charge-transfer-type insulator [16]. The size of the smallest energy gap was predicted to depend on the value of the onsite Coulomb repulsion U and the type of the magnetic configurations of the cubic phase: either ferromagnetic (FM) phase or one of the distorted antiferromagnetic (AFM) phases $[110]_1$ and $[110]_2$. As an example, for $U = 1$ eV the band structure of the AFM-$[110]_2$ phase showed the removal of some bands at the Γ point from the region near E_F, leading to the opening of an indirect gap smaller than 0.1 eV. When increasing U to 3 eV, both of the AFM-$[110]_2$ and FM phases' band structures showed the opening of a small direct gap slightly less than 1 eV near the Γ point, while for the AFM-$[110]_1$ phase the gap was found to be about 0.4 eV. This small gap was suggested to be opened between the N $2p$-type valence band and the majority-spin e_g bands of Cr, and hence CrN was interpreted in terms of a charge-transfer type insulator, even for small values of U. According to the calculations of Herwadkar *et al.*, the MIR band observed in our optical data at around 125 meV can be explained in terms of a charge transfer Δ from the N $2p$-type bands to the Cr $3d$-type bands. This would support the transport data, which proposed that CrN is located in the charge transfer insulator regime, close to the itinerant electron limit [10,11]. Furthermore, the band structure calculations [17] showed another energy gap at around 1.8 eV, opened between the minority spin N $2p$-type valence band and the minority-spin t_{2g} band at the X point. This could explain the high-energy band at around 1.5 eV observed in our data and the data of Zhang *et al.* Accordingly, we suggest that both the MIR band and the high-energy band could be explained in terms of a charge-transfer insulator rather than a Mott insulator. A charge gap of similar size was also observed for other $3d$ transition-metal compounds, like $Ni_{1-\delta}S$, $BaTiO_3$ and the family of the rare-earth (R) transition metal oxides (RMO_3, with $M =$ Sc, Ti, V, Cr, Mn, Fe, Co, Ni, and Cu), and interpreted in terms of a charge transfer between $2p$-type and $3d$-type states [27–29].
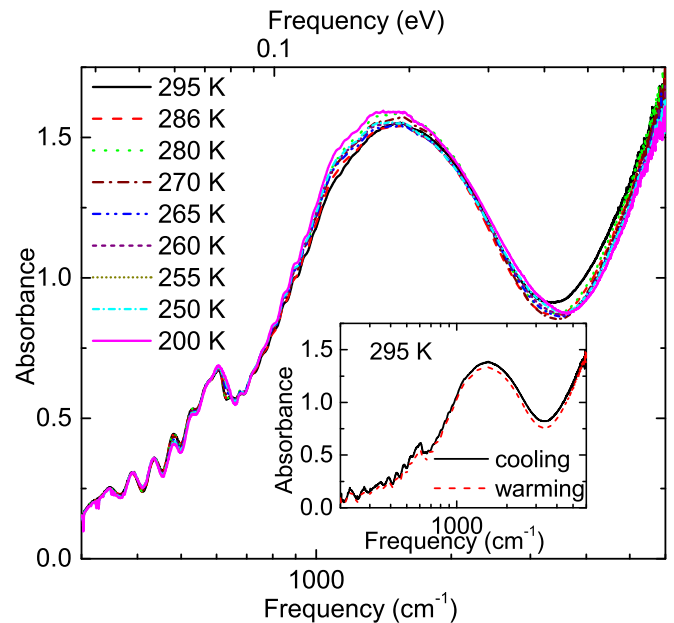

FIG. 2. Temperature-dependent absorbance of a polycrystalline CrN/CsI pellet at ambient pressure. Inset shows the absorbance spectra at room temperature before cooling down and after warming up.

B. Temperature-dependent optical spectra

Ambient-pressure absorbance spectra of CrN for several selected temperatures are displayed in Fig. 2 in the frequency range 0.025–0.868 eV (200–7000 cm^{-1}). The wiggles in the spectra are due to Fabry-Perot interferences due to multiple reflections within the sample. As the temperature is lowered, the absorption spectra do not show significant spectral changes below 0.062 eV (500 cm^{-1}), consistent with the electrical transport measurements which found an activated behavior for CrN for the temperature range below 400 K [10,11]. Additionally, the MIR absorption band shows only a slight shift to lower frequencies during cooling down, indicating that the temperature effect on the activation energy is very small. The major changes were observed in the phonon mode range, i.e., between 0.068 eV (550 cm^{-1}) and 0.083 eV (670 cm^{-1}). With decreasing temperature, the phonon mode shows a sudden broadening below 270 K, followed by a splitting during further cooling down, as depicted in Fig. 3(a). The changes in the phonon mode with temperature are illustrated by the normalized difference ΔA, defined as

$$\Delta A(\omega, T) = [A(\omega, T) - A(\omega, 300 \text{ K})]/A(\omega, 300 \text{ K}). \quad (1)$$

The temperature-dependent absorbance spectra and the corresponding normalized difference spectra $\Delta A(\omega, T)$ are shown in Fig. 3 in the upper and lower panels, respectively. With decreasing temperature, $\Delta A(\omega, T)$ has a slope of around zero for $T > 280$ K, while below 280 K the slope starts to change in the frequency range 0.068–0.083 eV (550–670 cm^{-1}). In particular, Fig. 3(c) shows that $\Delta A(\omega, T)$ clearly increases below 270 K during cooling, indicating the splitting of the phonon mode.

The broadening and splitting of the phonon mode at T_N are consistent with a symmetry lowering of the crystal structure
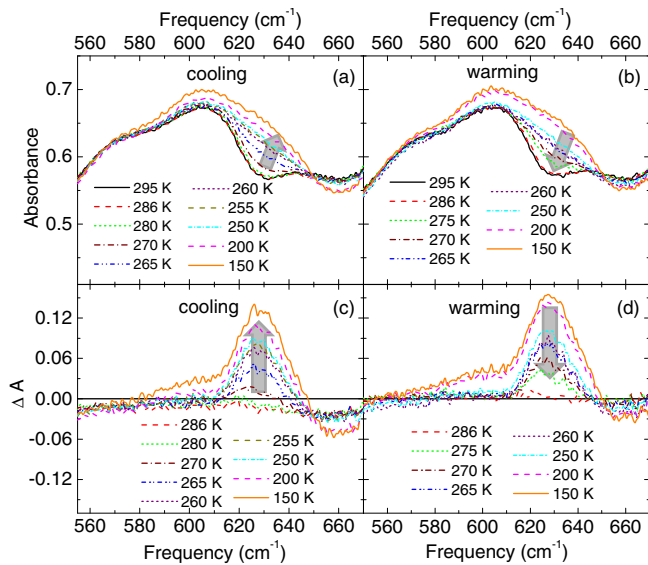
FIG. 3. The two panels (a) and (b) depict the absorbance of a CrN/CsI pellet as a function of temperature. The two panels (c) and (d) show the normalized difference $\Delta A(\omega, T)$ in the far infrared range, illustrating the evolution of the phonon mode as a function of temperature above and below the phase transition temperature. Block arrows illustrate the changes during cooling and warming.

from a cubic rock-salt structure with space group ($Fm3m$) to an orthorhombic phase with space group ($Pnma$) [6,7,30]. These structural changes are accompanied by a magnetic phase transition from a paramagnetic phase to an ordered antiferromagnetic phase at T_N as shown by several studies [5–8].

During warming up, $\Delta A(\omega, T)$ is basically flat above 275 K in the frequency range 0.068–0.083 eV (550–670 cm^{-1}) [see Fig. 3(d)], indicating the absence of any broadening or splitting of the phonon mode. The width of the so-obtained thermal hysteresis amounts to ≈ 5 K. The thermal hysteresis was observed in earlier studies, but with different values of the width depending on the N concentration [10–13,25]. Browne *et al.* [5] reported a hysteresis with a width of ≈ 3 K, which is close to our result, while Constantine *et al.* [25] found a higher value of ≈ 20 K. The thermal hysteresis indicates that the phase transition is of first order, as proposed earlier [5,25]. Furthermore, we note that the observed temperature-induced changes are reversible (see the inset of Fig. 2).

C. Pressure-dependent optical spectra

The room-temperature reflectance spectra of CrN for selected pressures between 0.2 and 4.5 GPa in the frequency range 0.02–0.086 eV (180–700 cm^{-1}) are depicted in Fig. 4. At the lowest pressure (≈ 0.2 GPa) a broad phonon mode and a shoulder are observed, consistent with our data at ambient conditions discussed above. The overall reflectance increases monotonically with increasing pressure, which might indicate a growth of spectral weight within the measured frequency range. However, we cannot exclude that the overall increase is due to pressure-induced changes in the surface flatness, since the CrN pellet is pressed on the diamond anvil. This
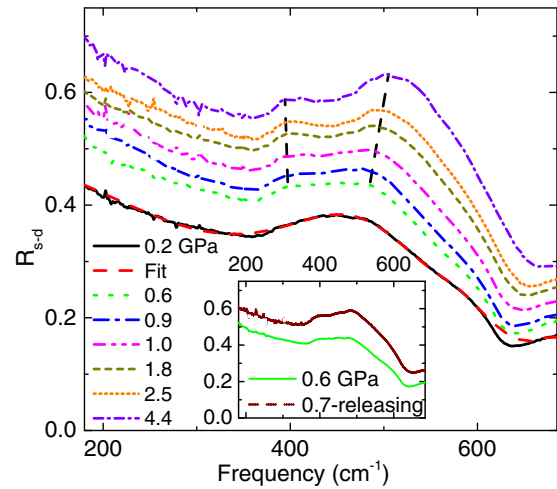

FIG. 4. Pressure-dependent reflectance of a pure CrN pellet at room temperature in the low-frequency range for several selected pressures between 0.2 and 4.4 GPa. The dashed red line is the fit of the reflectance spectrum at 0.2 GPa using the Lorentz model. The two dashed black lines illustrate the splitting of the phonon mode.

might also explain the rather high overall reflectance after pressure release at 0.7 GPa (see inset of Fig. 4). Nevertheless, the nonreversibility of the pressure-induced effects cannot be excluded as a possible reason for the discrepancy between the spectra at around 0.6 GPa during pressure increase and after pressure release.

The pressure-dependent phonon spectrum was analyzed by fitting with the Lorentz model. Hereby, the reflectance spectra were fitted according to the Fresnel equation for normal-incidence reflectivity taking into account the diamond-sample interface R_{s-d}. Further information about Fresnel equation for R_{s-d} is included in an earlier publication [31]. The phonon modes are described by two Lorentz functions. As an example, we show in Fig. 4 the fit of the reflectance spectrum at 0.2 GPa. Above 0.6 GPa an activation of a phonon mode at ≈ 50 meV occurs, which is directly seen in the reflectance spectra (see the dashed lines in Fig. 4). Therefore, an additional Lorentz term had to be included in the fit.

Based on the Lorentz fitting, the phonon frequencies were extracted and are plotted in Fig. 5 as a function of pressure. With increasing pressure, the phonon mode at ≈ 55 meV slightly shifts to higher energy, while the shoulder at ≈ 69 meV broadens. Furthermore, the activation of a phonon mode located at around 50 meV indicates a pressure-induced symmetry lowering of the crystal structure above 0.6 GPa. This finding supports the structural phase transition observed by Rivadulla *et al.* [9], from the cubic rock salt to an orthorhombic crystal structure at ≈ 1 GPa. Concomitant with the structural phase transition, a large reduction of the bulk modulus K_0 from 340(10) GPa for the cubic rock-salt phase to 243(10) GPa for the orthorhombic phase was reported; i.e., CrN softens under pressure.

IV. SUMMARY

In summary, the electronic and vibrational properties of polycrystalline CrN have been investigated by transmission
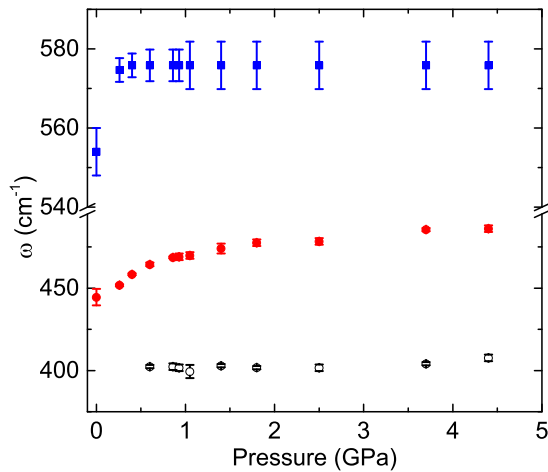
FIG. 5. Phonon frequencies as a function of pressure, obtained by fitting the reflectance spectra with the Lorentz model.

and reflection measurements in the infrared frequency range for temperatures between 300 and 150 K, and under high

pressure up to 4.5 GPa. At ambient conditions, the optical conductivity spectrum shows an optical phonon mode at ≈ 55 meV with a shoulder at ≈ 69 meV, a MIR absorption band at 123 ± 2 meV, and a high-energy absorption band at ≈ 1.5 eV. Both absorption bands can be related to charge transfer excitations, suggesting that CrN is a charge-transfer-type insulator. While cooling down, the phonon mode exhibits a sudden broadening and a splitting below T_N, which confirms the occurrence of the expected magnetostructural phase transition. This magnetostructural phase transition seems to occur also under pressure according to our pressure-dependent reflectance measurements, revealing the activation of a phonon mode at 0.6 GPa, in agreement with earlier studies.

[1] U. Wiklund, M. Bromark, M. Larsson, P. Hedenqist, and S. Hogmark, Surf. Coat. Technol. **91**, 57 (1997).

[2] C. Nouveau, M. A. Djouadi, O. Banakh, R. Sanjines, and F. Levy, Thin Solid Films **398-399**, 490 (2001).

[3] A. Neckel, Int. J. Quantum Chem. **23**, 1317 (1983).

[4] B. R. Zhao, L. Chen, H. L. Luo, M. D. Jack, and D. P. Mullin, Phys. Rev. B **29**, 6198 (1984).

[5] J. D. Browne, P. R. Liddell, R. Street, and T. Mills, Phys. Status Solidi A **1**, 715 (1970).

[6] L. M. Corliss, N. Elliott, and J. M. Hastings, Phys. Rev. **117**, 929 (1960).

[7] R. M. Ibberson and R. Cywinski, Physica B (Amsterdam, Neth.) **180-181**, 329 (1992).

[8] M. N. Eddine, F. Sayetat, and E. F. Bertaut, C. R. Seances Acad. Sci., Ser. B **269**, 574 (1969).

[9] F. Rivadulla, M. Banobre-Lopez, C. X. Quintela, A. Pineiro, V. Pardo, D. Baldomir, M. A. C. R. Lopez-Quintela, J. Rivas, C. A. Ramos, H. Salva, J. S. Zhou, and J. B. Goodennough, Nat. Mater. **8**, 947 (2009).

[10] C. X. Quintela, F. Rivadula, and J. Rivas, Appl. Phys. Lett. **94**, 152103 (2009).

[11] C. X. Quintela, J. P. Podkaminer, M. N. Luckyanova, T. R. Paudel, E. L. Thies, D. A. Hillsberry, D. A. Tenne, E. Y. Tsymbal, G. Chen, C. Eom, and F. Rivadula, Adv. Mater. **27**, 3032 (2015).

[12] P. S. Herle, M. S. Hedge, N. Y. Vasathacharya, S. Philip, M. V. R. Rao, and T. Sripathi, J. Solid State Chem. **134**, 120 (1997).

[13] D. Gall, C.-S. Shin, R. T. Haasch, I. Petrov, and J. E. Greene, J. Appl. Phys. **91**, 5882 (2002).

[14] C. X. Quintela, F. Rivadulla, and J. Rivas, Phys. Rev. B **82**, 245201 (2010).

[15] K. Inumaru, K. Koyama, N. Imo-oka, and S. Yamanaka, Phys. Rev. B **75**, 054416 (2007).

[16] M. Imada, A. Fujimori, and Y. Tokura, Rev. Mod. Phys. **70**, 1039 (1998).

[17] A. Herwadkar and W. R. L. Lambrecht, Phys. Rev. B **79**, 035125 (2009).

[18] P. A. Anderson, R. J. Kinsey, S. M. Durbin, A. Markwitz, V. J. Kennedy, A. Asavod, W. Gao, and R. J. Reeves, J. Appl. Phys. **98**, 043903 (2005).

[19] X. Y. Zhang and D. Gall, Phys. Rev. B **82**, 045116 (2010).

[20] M. Hirai, Y. Ueno, T. Suzuki, W. Jiang, C. Grigoriu, and K. Yatsuil, Jpn. J. Appl. Phys. **40**, 1052 (2001).

[21] D. B. Tanner, Phys. Rev. B **91**, 035123 (2015).

[22] K. Syassen, High Press. Res. **28**, 75 (2008).

[23] C. A. Kuntscher, S. Frank, A. Pashkin, M. Hoinkis, M. Klemm, M. Sing, S. Horn, and R. Claessen, Phys. Rev. B **74**, 184402 (2006).

[24] J. Ebad-Allah, L. Baldassarre, M. Sing, R. Claessen, V. A. M. Brabers, and C. A. Kuntscher, J. Phys. Condens. Matter **25**, 035602 (2013).

[25] C. Constantin, M. B. Haider, D. Ingram, and A. R. Smith, J. Appl. Phys. Lett. **85**, 6371 (2004).

[26] J. Shirahata, T. Ohori, H. Asami, T. Suzuki, T. Nakayama, H. Sematsu, and K. Niihara, Jpn. J. Appl. Phys. **50**, 01BE03 (2011).

[27] Ph. Ghosez, X. Gonze, Ph. Lambin, and J. P. Michenaud, Phys. Rev. B **51**, 6765 (1995).

[28] T. Arima, Y. Tokura, and J. B. Torrance, Phys. Rev. B **48**, 17006 (1993).

[29] H. Okamura, J. Naitoh, T. Nanba, M. Matoba, M. Nishioka, S. Anzai, I. Shimoyama, K. Fukui, H. Miura, H. Nakagawa, K. Nakagawa, and T. Kinoshita, Sol. Stat. Commun. **112**, 91 (1999).

[30] P. Hones, N. Martin, M. Regula, and F. Levy, J. Appl. Phys. **36**, 1023 (2003).

[31] J. Ebad-Allah, L. Baldassarre, M. Sing, R. Claessen, V. A. M. Brabers, and C. A. Kuntscher, J. Appl. Phys. **112**, 073524 (2013).